Gene expression is encoded in all parts of a co-evolving interacting gene regulatory structure

Jan Zrimec[1], Filip Buric[1], Azam Sheikh Muhammad[2], Rhongzen Chen[2], Vilhelm Verendel[2], Mats Töpel[3,4], Aleksej Zelezniak[1,5]*

1 - Department of Biology and Biological Engineering, Chalmers University of Technology, Kemivägen 10, SE-412 96, Gothenburg, Sweden

2 - Computer Science and Engineering, Chalmers University of Technology, Kemivägen 10, SE-412 96, Gothenburg, Sweden

3 - Department of Marine Sciences, University of Gothenburg, Box 461, SE-405 30, Gothenburg, Sweden

4 - Gothenburg Global Biodiversity Center (GGBC), Box 461, 40530 Gothenburg, Sweden

5 - Science for Life Laboratory, Tomtebodavägen 23a, SE-171 65, Stockholm, Sweden

* corresponding author (email: aleksej.zelezniak@chalmers.se)

Table of contents

Supplementary figures

A.

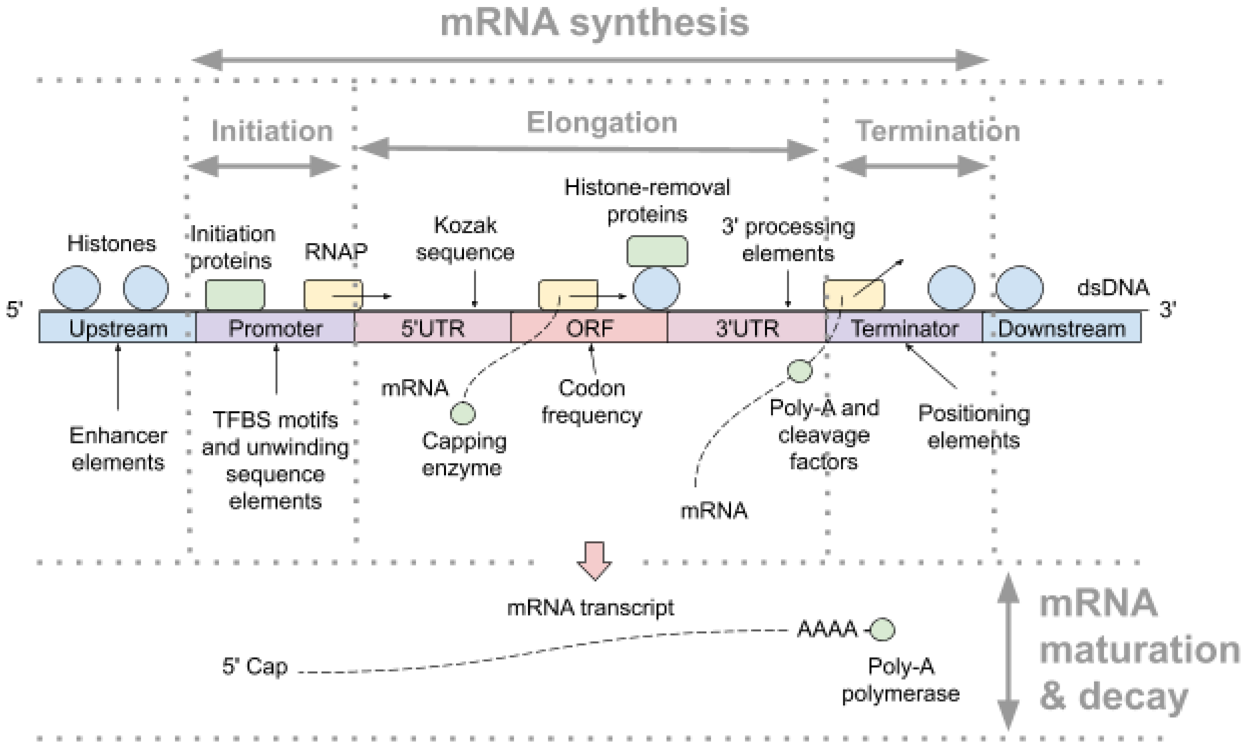

B.

Region	Promoter	5'UTR	Gene (CDS)	3'UTR	Terminator
$\boldsymbol{R^2}$	0.46[a]	0.52[b]	0.55[c]	>0.16[d]	

[a] Not genome-wide [1]

[b] Expanded to 0.62 with deep learning [2,3]

[c] Target variable was mRNA half-life, up to 0.59 achieved with extra features [4]

[d] Estimated here based on multiple studies [5,6]

C.

Region	Promoter	5'UTR	CDS	3'UTR	Terminator
Regulatory signals	- Core promoter [7] - TFBS [8] - enhancers [9]	Kozak sequence [2,10]	Codon usage [11,12]	3' processing elements: - A/T-rich sites [13] - Positioning element [14] - TA-rich efficiency el. [5]	
	Nucleosome positioning [6,12,15]				
Size	1000 bp	300 bp	~300-3000 bp	350 bp	500 bp
Positioning	to TSS	to START [2]	whole	to TTS [13]	from TTS
Data types	sequence	sequence, variables (2)	variables (67)	sequence, variables (2)	sequence
Sequence data	yes	yes	no	yes	yes
Variable types	/	length, GC content [4]	codon freq., length, GC of each wobble pos. [1,16]	length, GC content [4]	/

Figure S1-1. Schematic overview of published knowledge on the gene regulatory structure in *Saccharomyces cerevisiae*. (A) The molecular processes: schematic diagram of mRNA transcription in eukaryotes, detailing separate optimized processes, that form a fine-tuned regulatory system which spans mRNA synthesis, maturation and decay [12]. (B) The information content: overview of the approximate amount of information on gene expression levels that is encoded in each separate region according to published studies. (C) The regulatory system: overview of the known regulatory signals that contain information on gene expression, as well as the sequence parameters and variables used to model and predict gene expression levels in the present study. UTR denotes untranslated regions, ORF open reading frame, CDS coding sequence, TFBS transcription factor binding sites, TSS transcription start site, TTS transcription termination site.

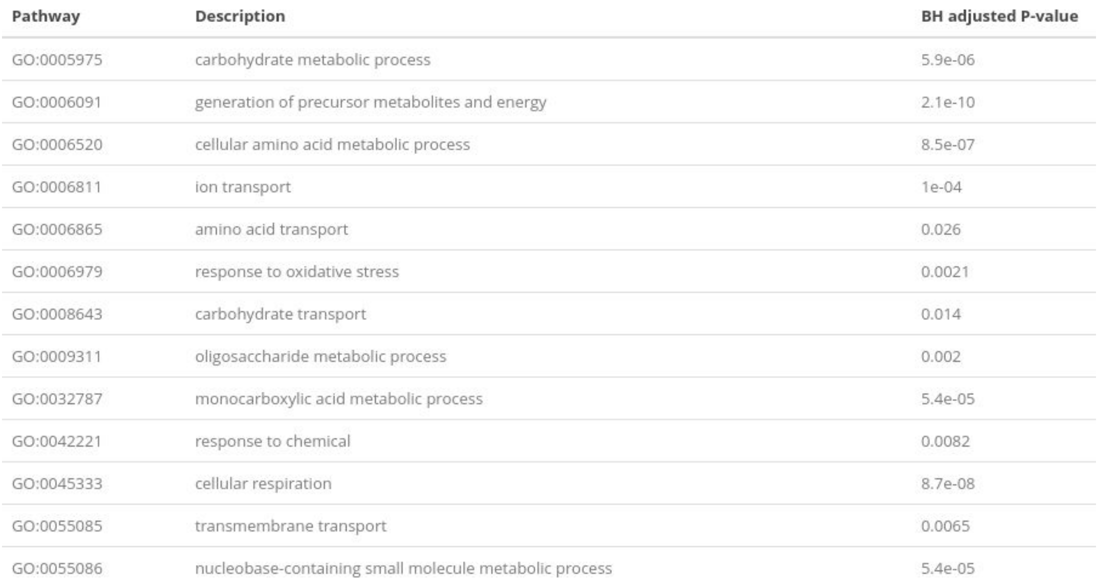

Pathway	Description	BH adjusted P-value
GO:0005975	carbohydrate metabolic process	5.9e-06
GO:0006091	generation of precursor metabolites and energy	2.1e-10
GO:0006520	cellular amino acid metabolic process	8.5e-07
GO:0006811	ion transport	1e-04
GO:0006865	amino acid transport	0.026
GO:0006979	response to oxidative stress	0.0021
GO:0008643	carbohydrate transport	0.014
GO:0009311	oligosaccharide metabolic process	0.002
GO:0032787	monocarboxylic acid metabolic process	5.4e-05
GO:0042221	response to chemical	0.0082
GO:0045333	cellular respiration	8.7e-08
GO:0055085	transmembrane transport	0.0065
GO:0055086	nucleobase-containing small molecule metabolic process	5.4e-05

Figure S1-2. Enrichment analysis of gene ontology terms [17,18] in the most variable genes across the entire range of biological conditions (*RSD* > 1).

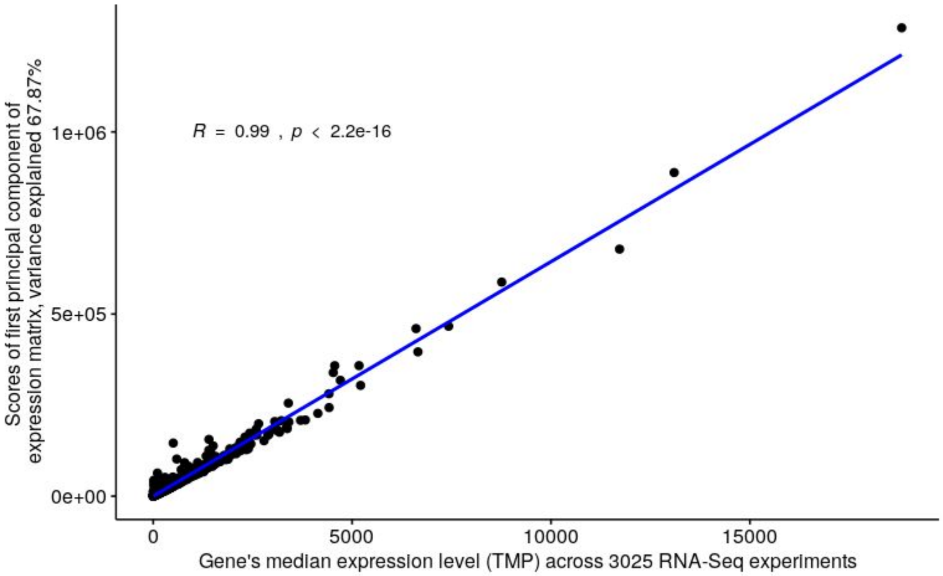

Figure S1-3. Median expression levels are representative of a gene's overall expression level across thousands of experiments, based on correlation analysis of the first principal component and median values of the entire matrix of mRNA counts (Pearson's $r = 0.99$, p-value < 2e-16). Line denotes least squares fit.

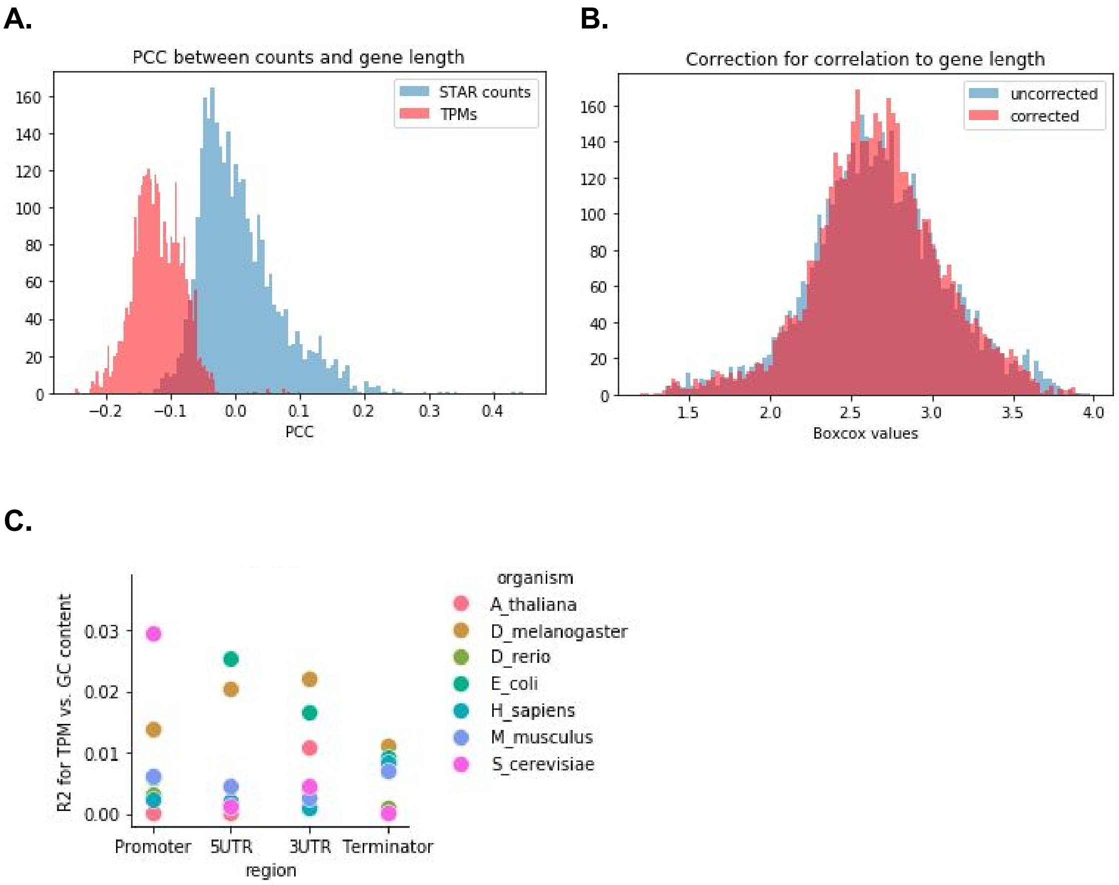

Figure S1-4. Overview for RNA-seq data processing with *Saccharomyces cerevisiae*. (A) A detectable level of correlation (above 0.1) was observed between TPM transformed mRNA counts and gene (CDS) length. "PCC" denotes Pearson correlation coefficient. (B) Correction of the TPM target variable, by regressing out gene (CDS) length values, retained all information as the original uncorrected TPM values (Pearson's *r* = 0.96, *p*-value < 1e-16). (C) Overall GC content of regulatory regions was not predictive of gene expression levels, as the coefficient of determination (R^2) between gene expression values and GC content was below 3% for all model organisms.

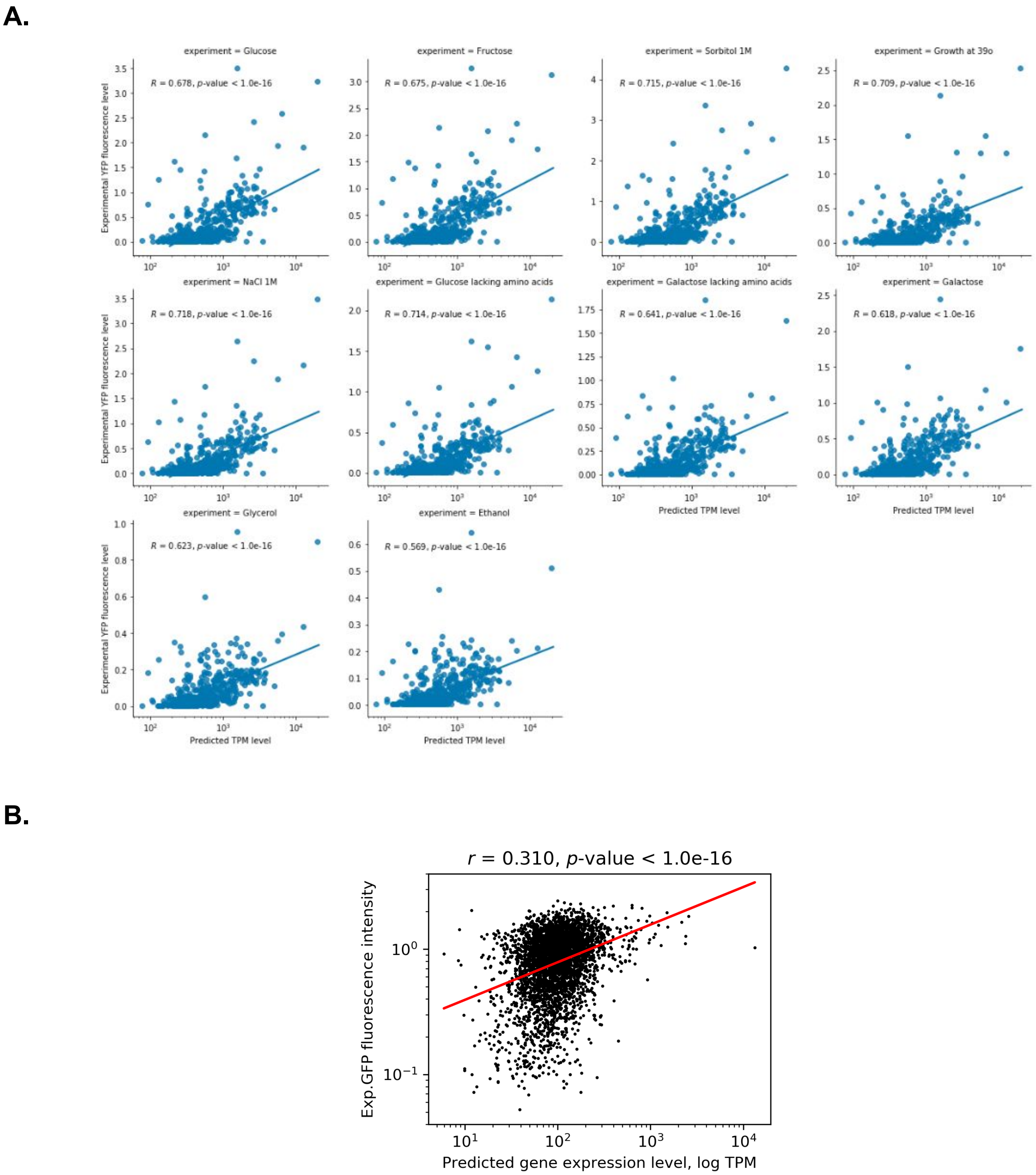

Figure S1-5. Model predictions are highly correlated with published experiments. (A) Experimental fluorescence measurements [19] versus predicted expression levels across 10 conditions. (B) Experimental fluorescence measurements [20] versus predicted expression levels. All lines denote least squares fit.

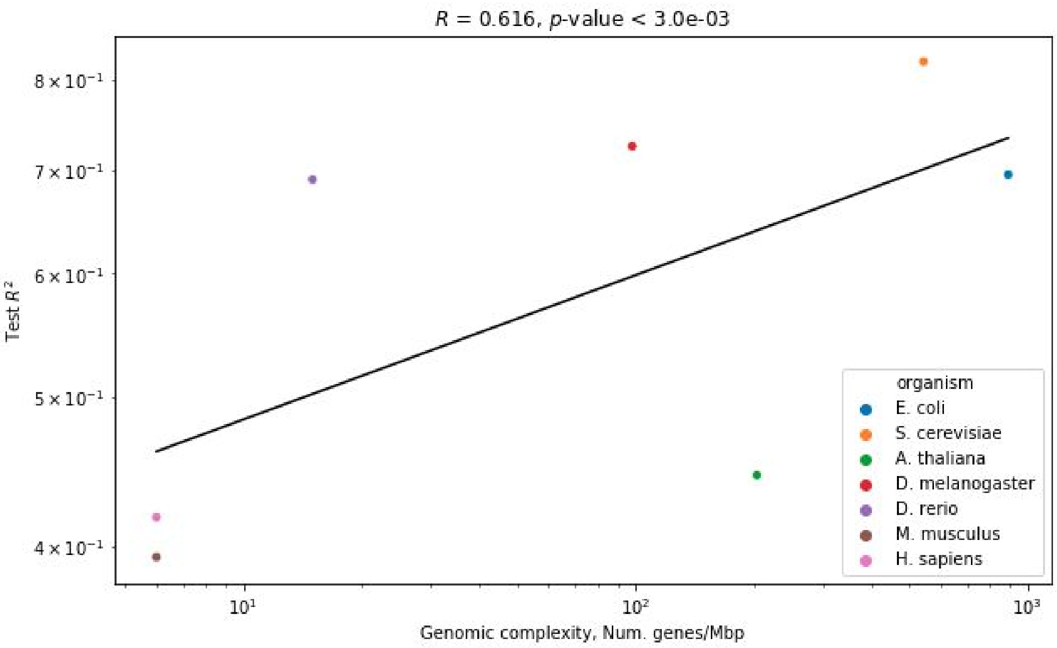

Figure S1-6. Correlation analysis between the predictive accuracy of deep learning models (R^2_{test}) and the genomic complexity of all model organisms. Line denotes least squares fit.

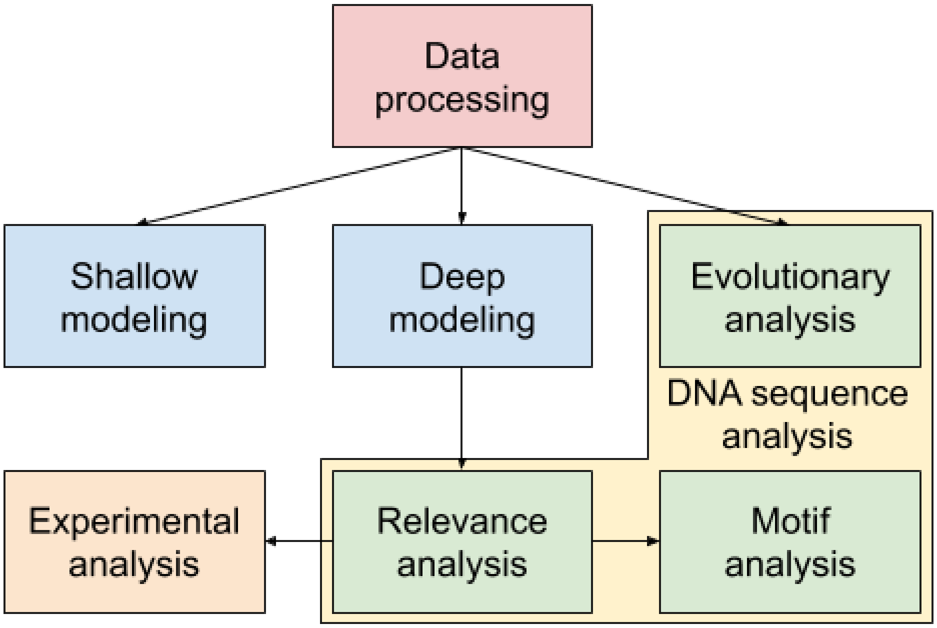

Figure S1-7. Overview of computational and experimental pipelines.

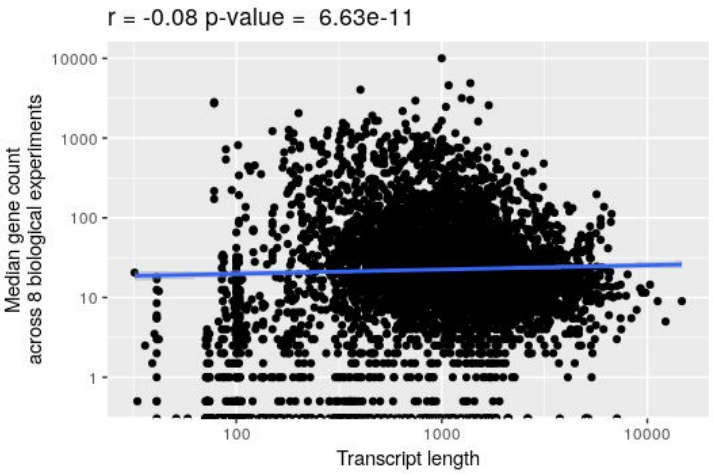

Figure S1-8. Correlation analysis between the gene length and the median expression level across experiments per gene, using data from whole molecule RNA-seq with the Oxford Nanopore MinION [21]. Line denotes least squares fit.

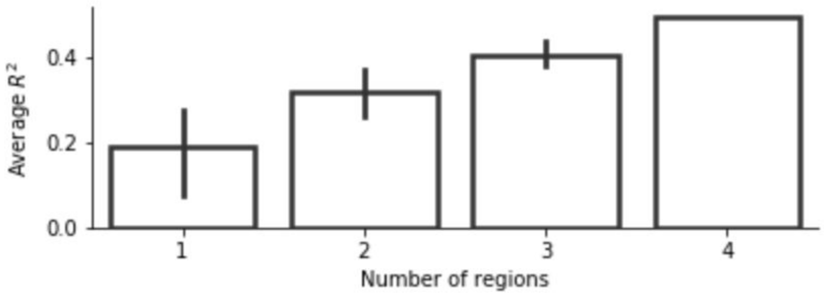

Figure S2-1. Effect of combinations of *cis*-regulatory regions on prediction of gene expression levels. The mean and 95% confidence intervals of R^2_{test} at different amounts of regulatory regions are shown.

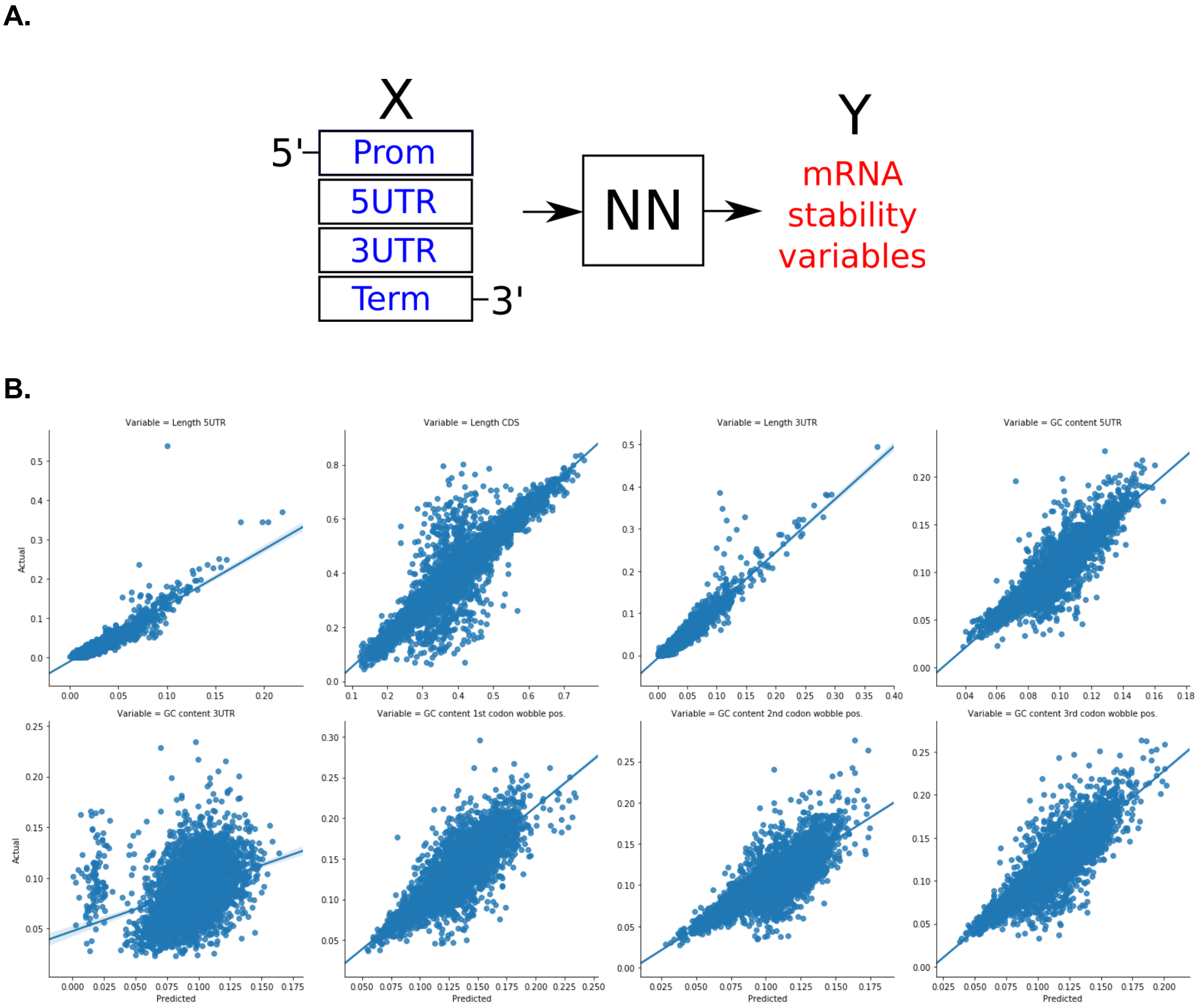

Figure S2-2. A CNN was built (A) that could predict nearly 80% of the variation of mRNA stability variables based on input regulatory sequences (R^2_{test} = 0.78). (B) Plots of actual versus predicted stability variables are shown, with individual R^2_{test} values of 0.788, 0.782, 0.864, 0.738, 0.146, 0.682, 0.645 and 0.684, respectively. All lines denote least squares fit.

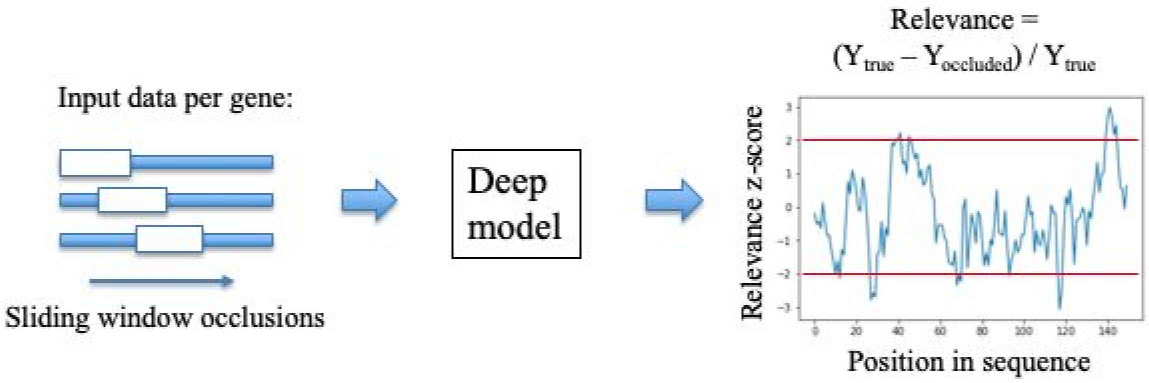

Figure S3-1. Schematic overview of the implemented occlusion relevance approach [22,23].

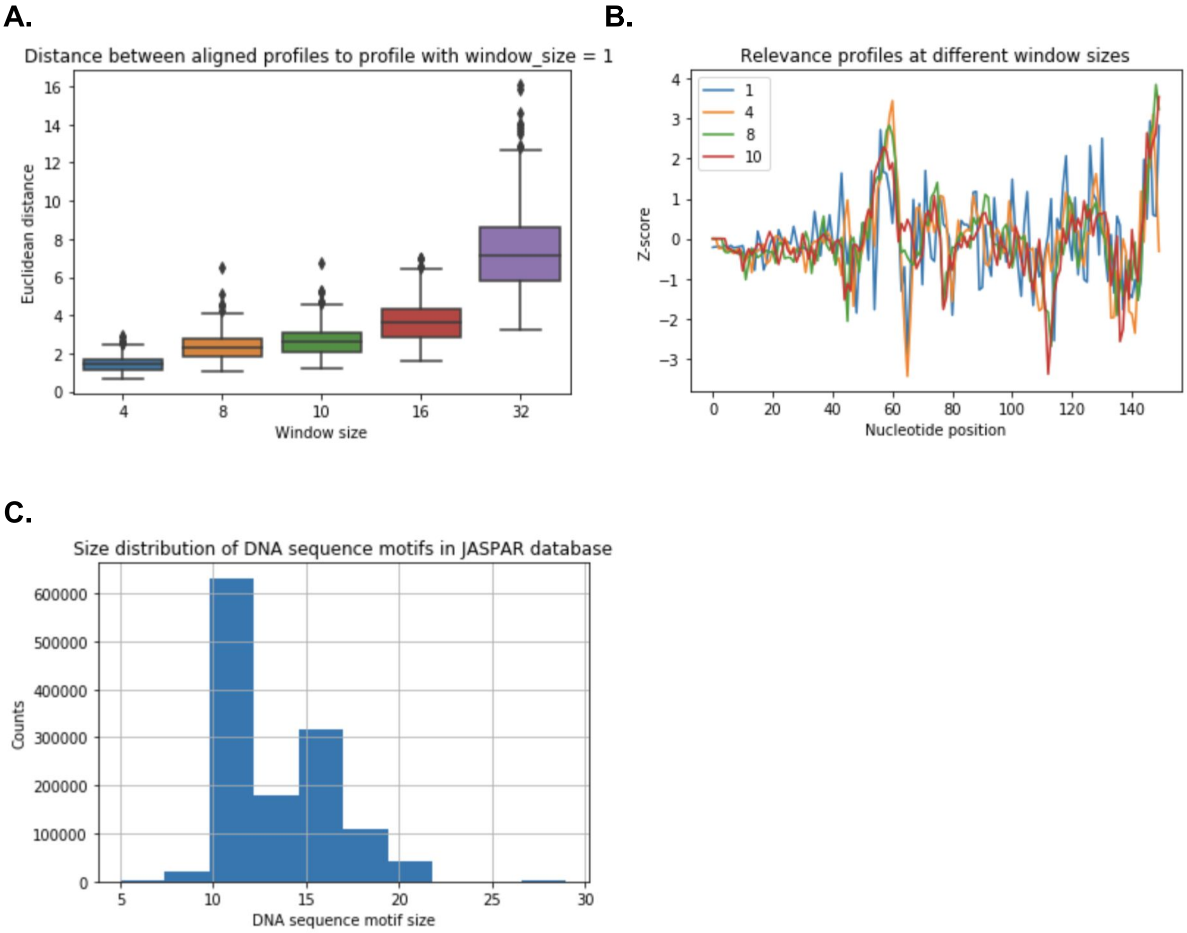

Figure S3-2. Analysis of different occlusion window sizes. (A) Euclidean distance between aligned profiles of sizes larger than 1 to the profiles with window size 1. FastDTW alignment method used [24]. (B) An example of the relevance profile with 150bps of a specific promoter region at different window sizes. (C) Size distribution of DNA sequence motifs in JASPAR database (sites file: http://jaspar.genereg.net/download/sites.tar.gz). Considering that over 98% of DNA sequence motifs are 10 bps or larger, the analysis suggested that a window size of 10 was a good choice to recover the relevance of true DNA sequence motifs, whilst retaining the relevant information obtainable with the smaller window sizes.

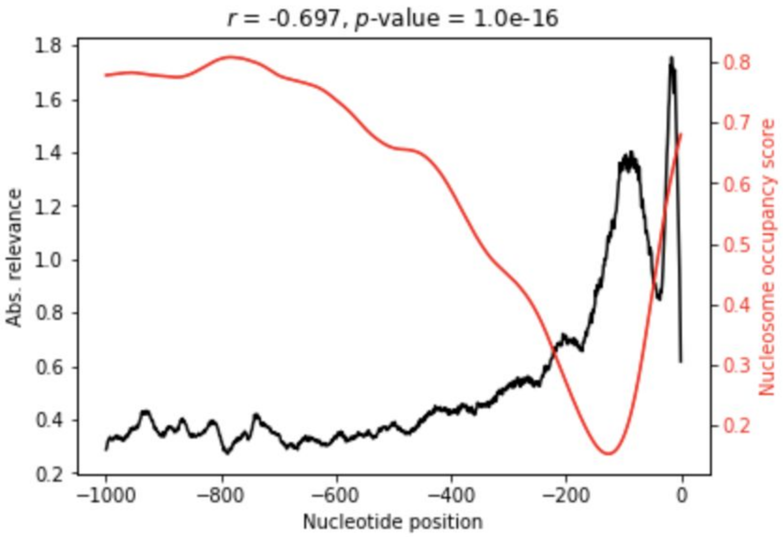

Figure S3-3. Strong correlation of absolute relevance in promoter regions and published nucleosome occupancy scores [25] for TFIID regulated genes [26], which were enriched (Fisher's exact test *p*-value < 1e-16) in the *S. cerevisiae* dataset.

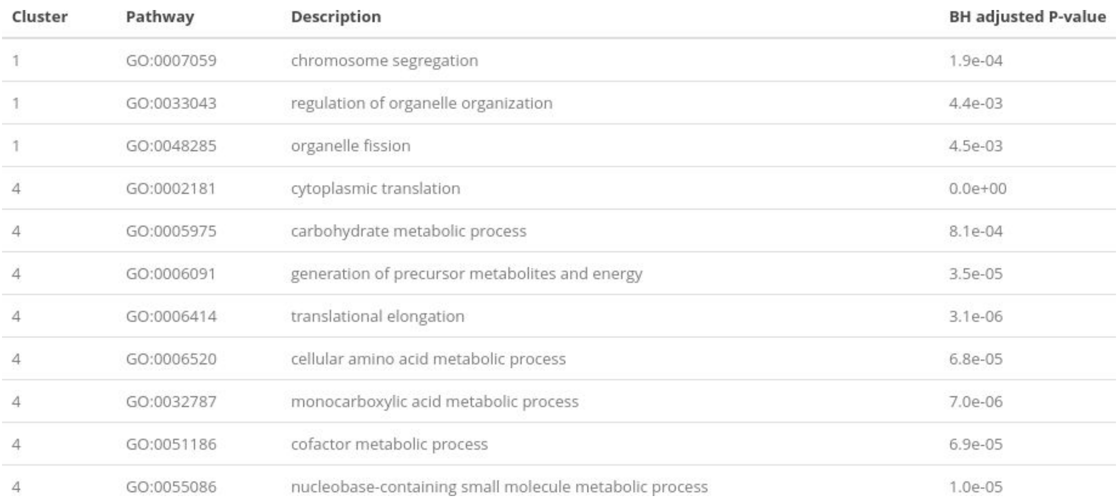

Cluster	Pathway	Description	BH adjusted P-value
1	GO:0007059	chromosome segregation	1.9e-04
1	GO:0033043	regulation of organelle organization	4.4e-03
1	GO:0048285	organelle fission	4.5e-03
4	GO:0002181	cytoplasmic translation	0.0e+00
4	GO:0005975	carbohydrate metabolic process	8.1e-04
4	GO:0006091	generation of precursor metabolites and energy	3.5e-05
4	GO:0006414	translational elongation	3.1e-06
4	GO:0006520	cellular amino acid metabolic process	6.8e-05
4	GO:0032787	monocarboxylic acid metabolic process	7.0e-06
4	GO:0051186	cofactor metabolic process	6.9e-05
4	GO:0055086	nucleobase-containing small molecule metabolic process	1.0e-05

Figure S3-4. Enrichment analysis of gene ontology terms [17,18] in Cluster 4 (with high expressed genes) of the clustered relevance profiles.

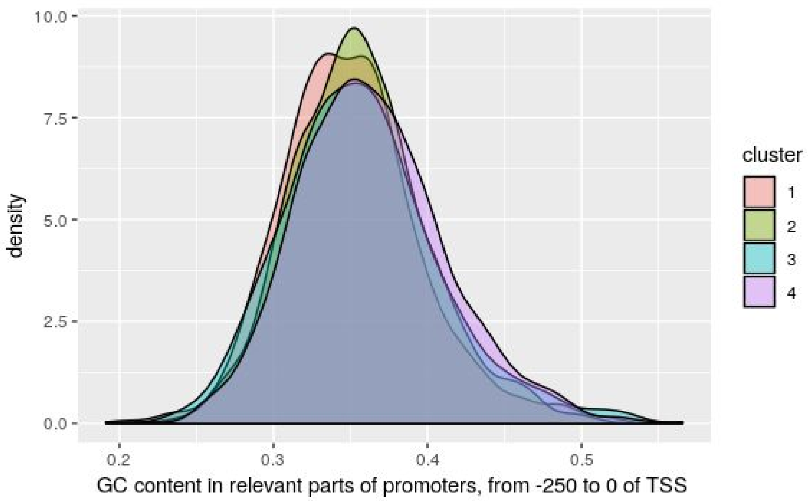

Figure S3-5. Clusters of relevance scores are independent of the DNA nucleotide composition.

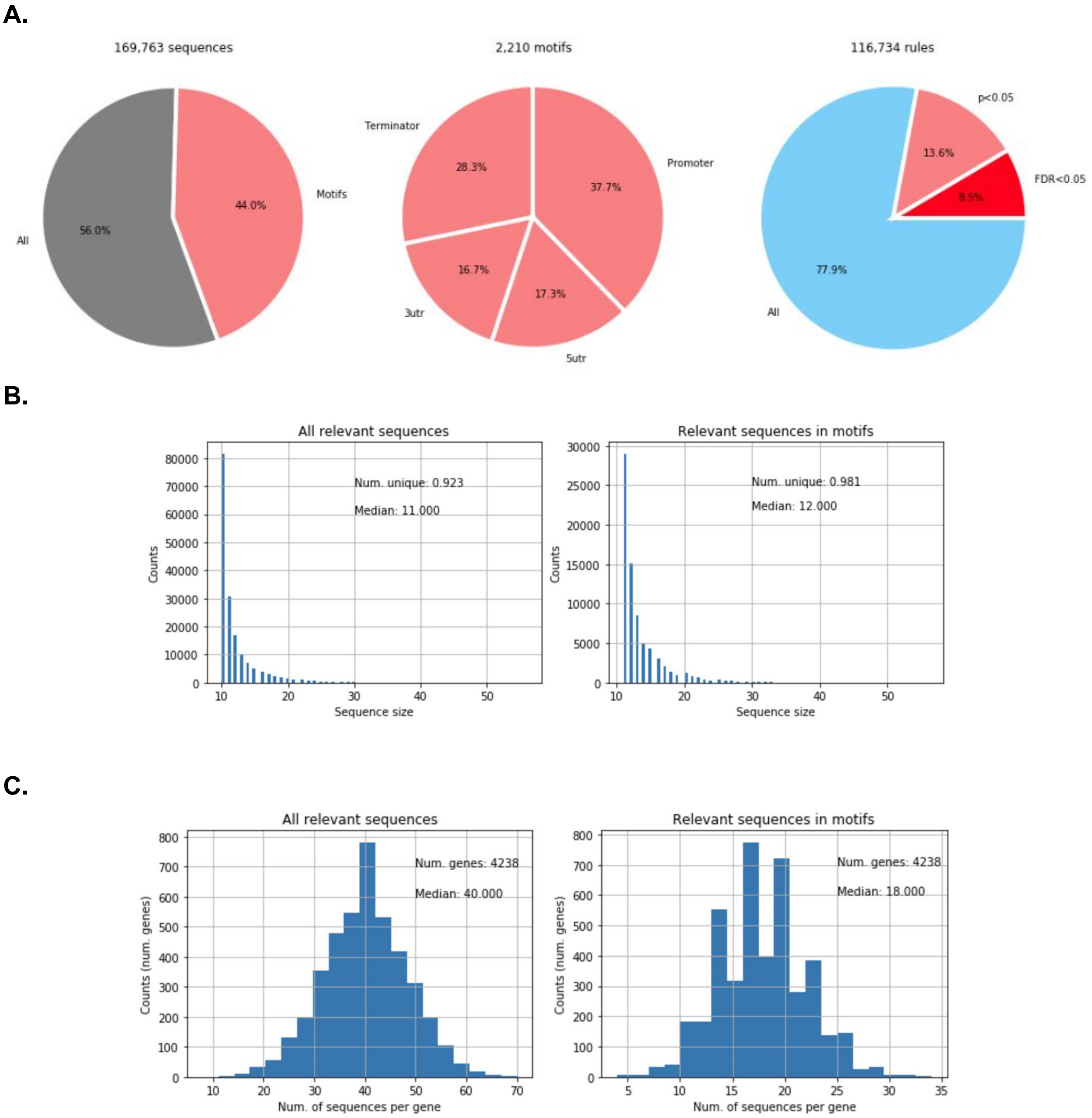

Figure S3-6. Analysis of significantly relevant DNA sequences. (A) 169,763 DNA sequences with significant relevance scores (exceeding 95% of range of values, i.e. ± 2 standard deviations) were extracted from the relevance profiles and used to construct regulatory DNA motifs and motif co-occurrence rules. Motif distributions across the *cis*-regulatory regions are shown. (B) Distribution of sizes of all relevant sequences and only those used for constructing the motifs (74,728 at 80% sequence identity cutoff, see Table S3-2). (C) Similarly, distribution of the amount of relevant sequences per gene showed good coverage of the whole set of genes with the extracted regulatory DNA motifs.

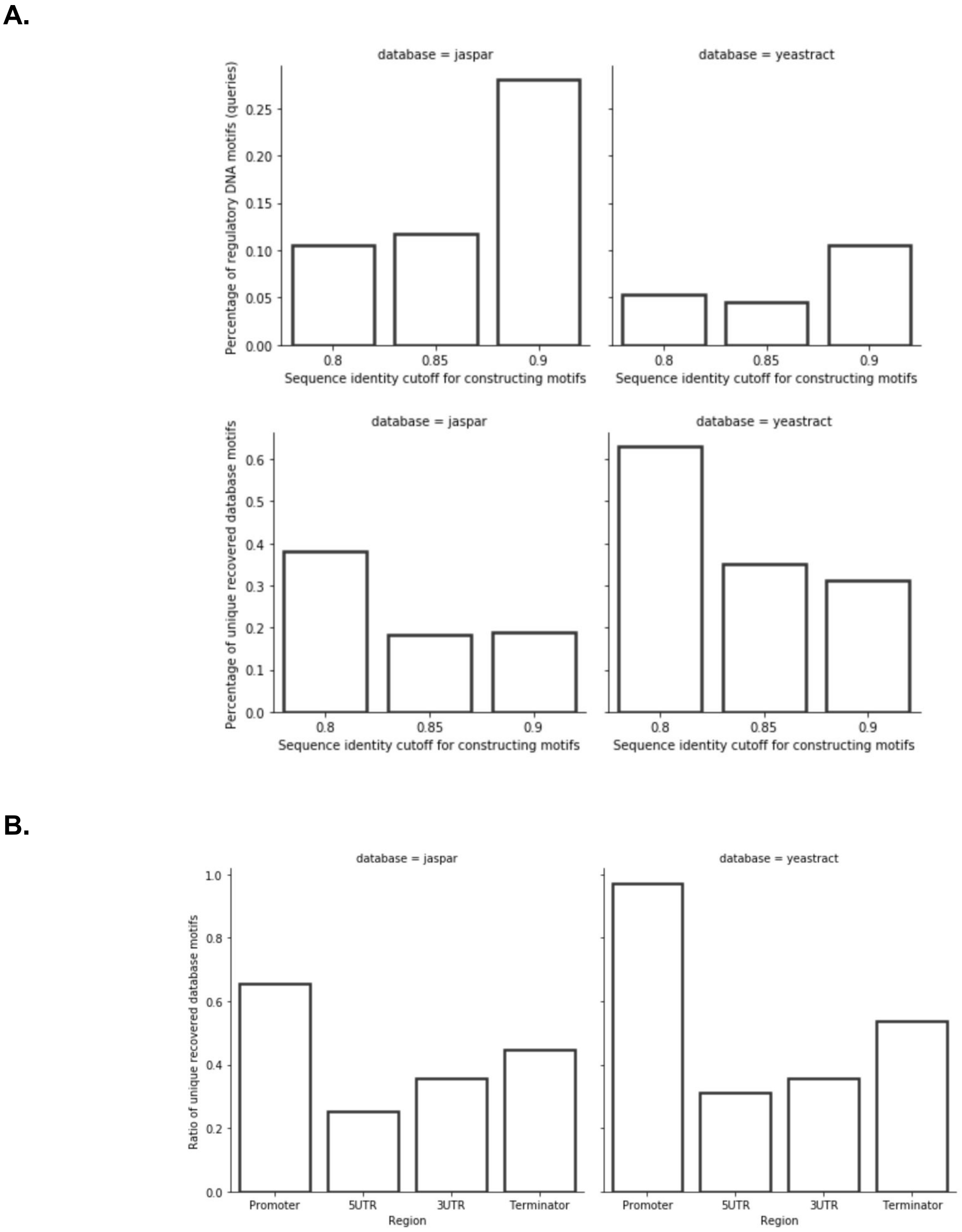

Figure S3-7. Comparison of constructed regulatory DNA motifs to JASPAR [27] and Yeastract [28] databases. (A) Although the number of regulatory DNA motifs that are significantly (BH adj. *p*-value < 0.05) similar to ones in databases increases with the increasing sequence identity cutoff used to construct the motifs, the number of unique recovered database motifs decreases, with the exception at the sequence identity cutoff of 0.85 with the Yeastract database. (B) Distribution of significant (BH adj. *p*-value < 0.05) motif hits from the JASPAR [27] and Yeastract [28] databases according to the regulatory regions, where the constructed regulatory motif queries were obtained.

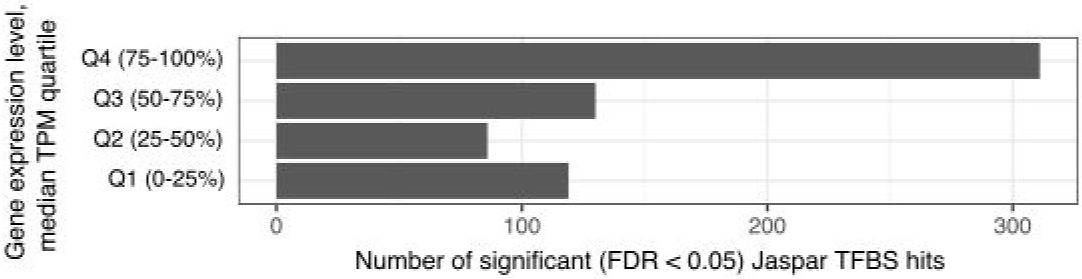

Figure S3-8. Enrichment of known yeast TFBS from the Jaspar database [27] in promoters of *Saccharomyces cerevisiae* genes, which were binned into quartiles based on median expression levels.

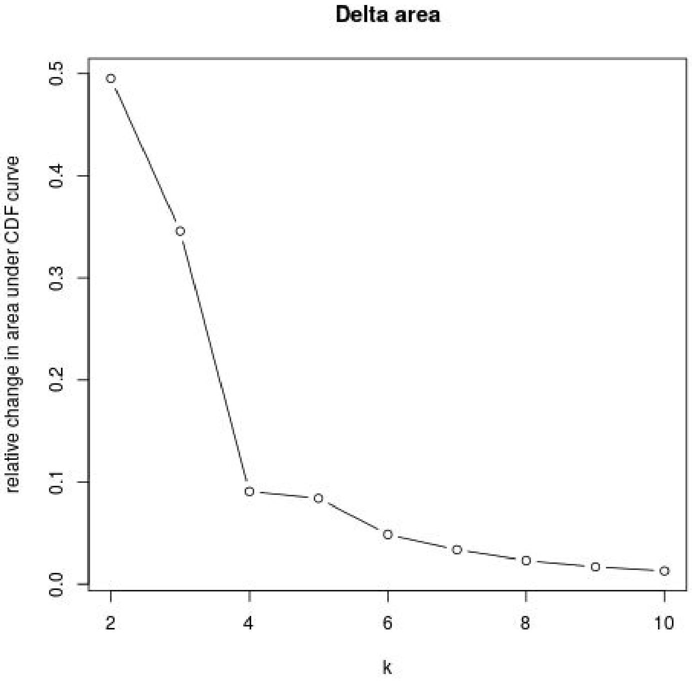

Figure S3-9. For clustering of relevance profiles the optimal amount of clusters *k* was determined at 4 (Methods).

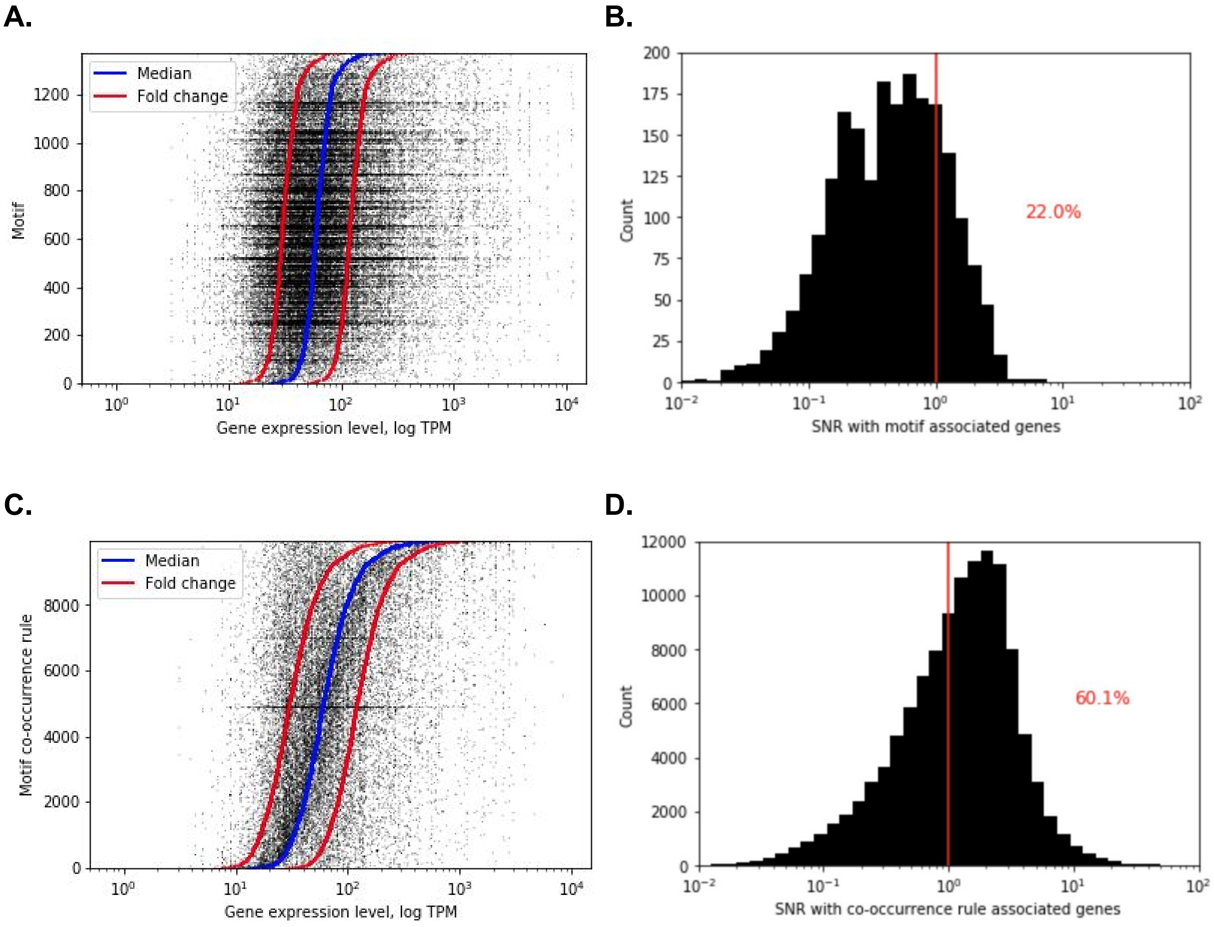

Figure S4-1. The range and precision of gene expression regulation with regulatory DNA motifs and motif co-occurrence rules. (A) Expression levels of genes associated with single motifs. (B) Distribution of the signal-to-noise ratio (*SNR*) of expression levels of genes associated with single motifs. Red line denotes an *SNR* of 1. (C) Expression levels of genes associated with motif co-occurrence rules. (D) Distribution of the signal-to-noise ratio (*SNR*) of expression levels of genes associated with motif co-occurrence rules. Red line denotes a *SNR* of 1.

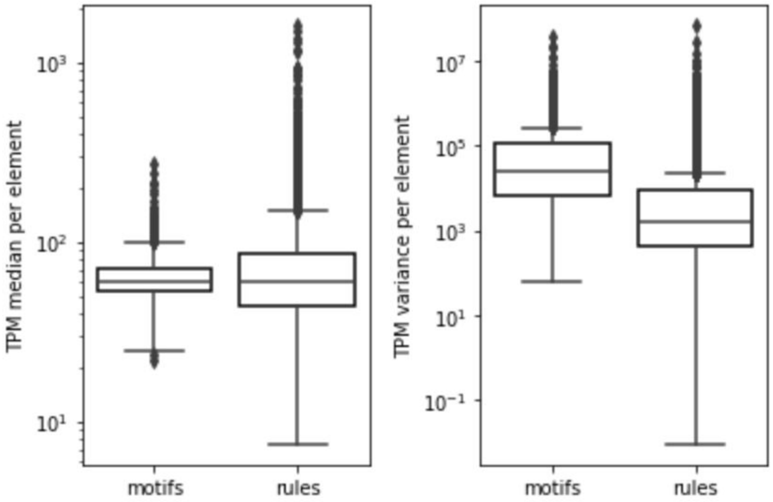

Figure S4-2. Median and variance of gene expression levels with genes associated with single motifs or motif co-occurrence rules.

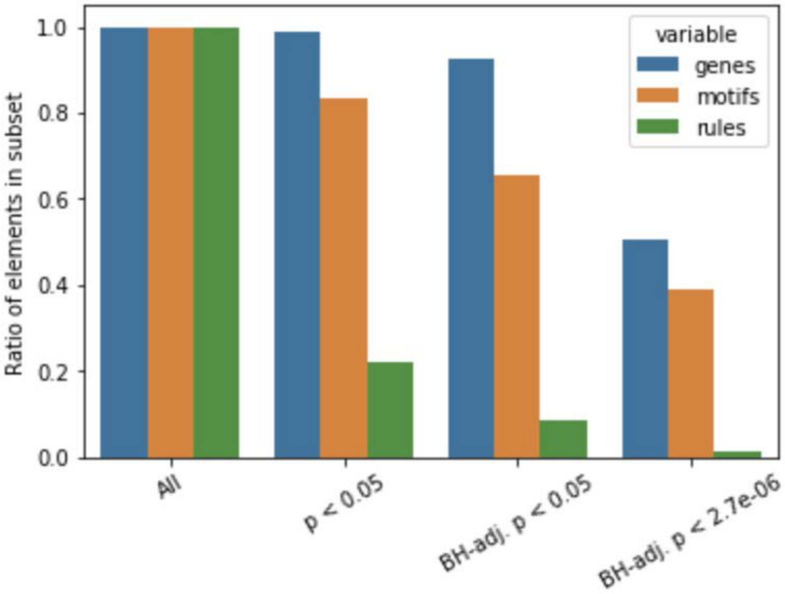

Figure S4-3. Ratio of retained elements: unique genes, motifs and rules, with increasing statistical stringency (Fig 4B).

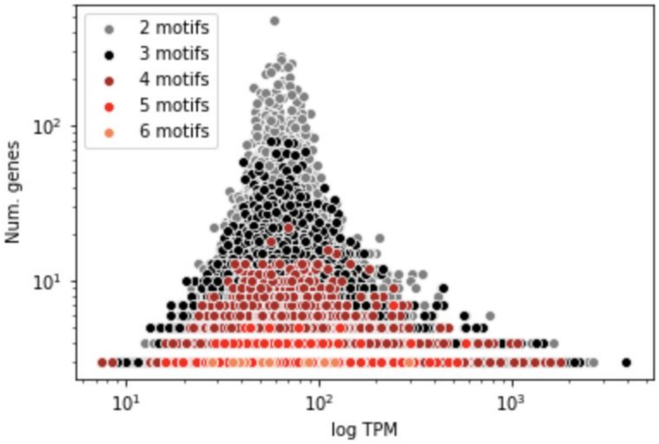

Figure S4-4. The number of co-occurring motifs and the amount of genes in a rule versus the average expression level across genes defined by that rule.

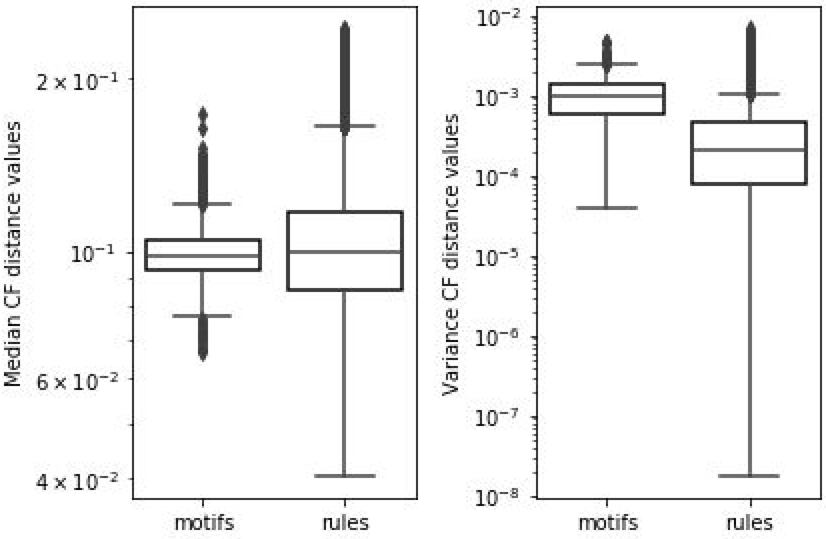

Fig S4-5. Median and variance of Euclidean distances between codon frequencies within genes defined by single motifs or motif co-occurrences.

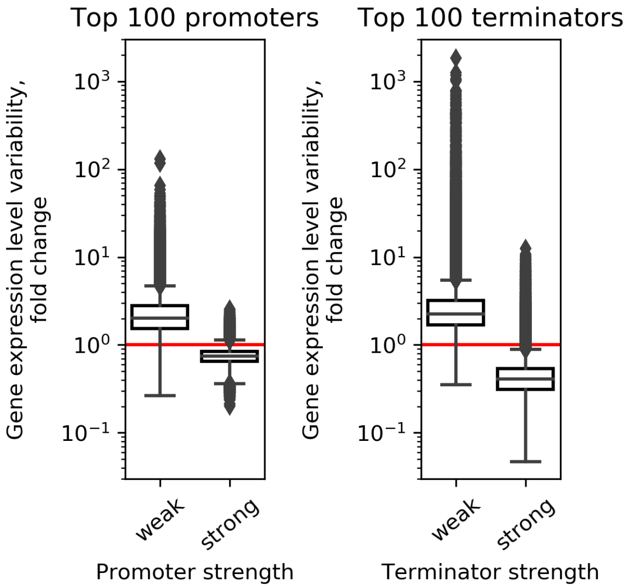

Figure S5-1. Variation of gene expression with strong and weak regulatory regions, represented by the selection of 100 top and bottom sorted constructs. (A) Native promoters combined with different terminators. (B) Native terminators combined with different promoters.

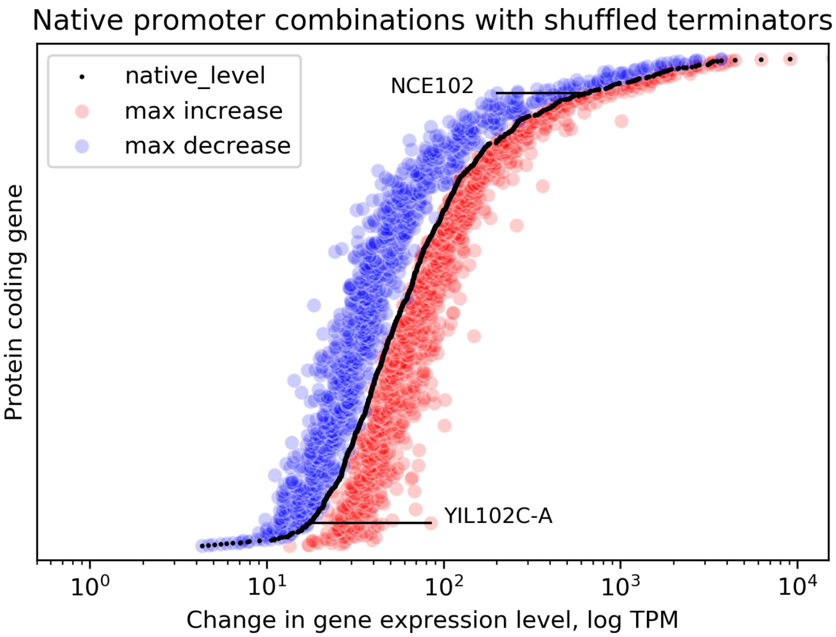

Figure S5-2. Evaluation of the effect of removing high-order sequence information (ie. regulatory grammar) by randomly shuffling the regulatory DNA whilst preserving dinucleotide frequencies (Altschul and Erickson 1985). On average, these constructs achieved a 1.4 -fold change in either direction of expression levels and a dynamic range below 1 order of magnitude (6.3 -fold range with YIL102C-A).

Supplementary Tables

Table S1-1. Overview of data and genomic features across the model organisms.

Organism	**Common name**	**Num. coding genes**	**Genome size (bps)**	**Coding gene density**	**Num. RNAseq datasets used**	**Num. genes with all regions available**
E. coli	Bacteria	4,140	4,641,652	892	355	2665
S. cerevisiae	Yeast	6,600	12,157,105	543	3025	5112
A. thaliana	Plant	27,655	135,670,229	204	5602	22569
D. melanogaster	Fruitfly	13,931	142,573,024	98	4410	13317
D. rerio	Fish	25,592	1,674,207,132	15	1084	17526
M. musculus	Mouse	22,604	3,486,944,526	6	2365	20244
H. sapiens	Human	20,465	3,609,003,417	6	4282	18016
Total	/	120,987	/	/	21,123	99,449
Average	/	17,284	1,295,028,155	252	3,018	14,207

Table S1-2. Overview of RNA-seq data across the model organisms.

Organism	**Num. active genes TPM_median > 5**	**Num. genes RSD < 3**	**Num. genes RSD < 2**	**Num. genes RSD < 1**
E. coli (K12)	2,154	2,012	1,737	932
S. cerevisiae	4,975	4,917	4,804	4,238
A. thaliana	13,814	13,737	13,510	11,719
D. rerio	7,173	7,050	6,719	4,686
D. melanogaster	9,772	9,643	9,227	5,297
M. musculus	9,951	9,785	9,370	6,585
H. sapiens	9,437	9,308	8,893	6,279
Total	57,276	56,452	54,260	39,736
Average	8,182	8,065	7,751	5,677
Relative all	0.644	0.979	0.947	0.665
Relative Prokarya	0.808	0.934	0.806	0.433
Relative Yeast	0.973	0.988	0.966	0.852
Relative Eukarya	0.616	0.987	0.951	0.704

Table S1-3. Results of deep modeling across the model organisms.

Organism	***RSD* cutoff**	**Box-Cox lambda**	**Train *R*^{2}**	**Validation *R*^{2}**	**Test *R*^{2}**
E. coli	*2*	-0.147	0.778	0.645	0.695
S. cerevisiae	*1*	0.220	0.841	0.87	0.822
A. thaliana	*1*	0.200	0.532	0.424	0.445
D. rerio	*1*	0.220	0.771	0.709	0.725
D. melanogaster	*1*	0.270	0.753	0.699	0.69
M. musculus	*1*	0.120	0.408	0.44	0.394
H. sapiens	*1*	0.220	0.466	0.418	0.418
Average	/	/	0.650	0.601	0.598

Table S1-4. Overview of the genomic data resources.

Organism	Strain	Model webpage	Ensembl web	Assembly
E. coli	K-12 MG1655	https://ecocyc.org/	http://bacteria.ensembl.org/Escherichia_coli_str_k_12_substr_mg1655/Info/Index	ASM584v2
S. cerevisiae	S288C	https://www.yeastgenome.org/	http://fungi.ensembl.org/Saccharomyces_cerevisiae/Info/Index	R64-1-1
A. thaliana		https://www.arabidopsis.org/	http://plants.ensembl.org/Arabidopsis_thaliana/Info/Index	TAIR10
D. rerio		https://zfin.org/	http://www.ensembl.org/Danio_rerio/Info/Index	GRCz11
D. melanogaster		http://flybase.org/	http://www.ensembl.org/Drosophila_melanogaster/Info/Index	BDGP6
M. musculus		http://www.informatics.jax.org/	http://www.ensembl.org/Mus_musculus/Info/Index	GRCm38
H. sapiens		https://www.ncbi.nlm.nih.gov/projects/genome/guide/human/	http://www.ensembl.org/Homo_sapiens/Info/Index?db=core	GRCh38

Table S1-5. Correlations between mRNA stability variables.

Variable 1	Variable 2	Pearson's *r*	*p*-value	R^2
len3u	gc_3u	0.239873	1.57E-56	0.057539
gc_c1	gc_c3	0.180456	2.38E-32	0.032564
len_5u	gc_c2	0.145716	1.51E-21	0.021233
gc_5u	gc_c3	0.142965	8.57E-21	0.020439
len_5u	len_cd	0.119115	7.26E-15	0.014188
gc_3u	gc_c3	0.109343	9.50E-13	0.011956
len_5u	gc_5u	0.077692	4.11E-07	0.006036
gc_c2	gc_c3	0.072511	2.30E-06	0.005258
gc_c1	gc_c2	0.066578	1.44E-05	0.004433
gc_3u	gc_c1	0.058565	1.36E-04	0.00343
len3u	gc_c2	0.041629	6.72E-03	0.001733
gc_5u	gc_3u	0.040962	7.65E-03	0.001678
len_cd	gc_5u	0.037118	1.57E-02	0.001378
gc_5u	gc_c1	0.026558	8.39E-02	0.000705
len_5u	len3u	0.011822	4.42E-01	0.00014
gc_5u	gc_c2	-0.008987	5.59E-01	0.000081
gc_3u	gc_c2	-0.015623	3.09E-01	0.000244
len_5u	gc_3u	-0.017595	2.52E-01	0.00031
len3u	gc_c1	-0.021041	1.71E-01	0.000443
len3u	gc_c3	-0.032953	3.19E-02	0.001086
len3u	gc_5u	-0.041471	6.93E-03	0.00172
len_5u	gc_c3	-0.04148	6.92E-03	0.001721
len_cd	gc_c2	-0.051434	8.09E-04	0.002646
len_cd	gc_3u	-0.051623	7.74E-04	0.002665
len_5u	gc_c1	-0.070484	4.37E-06	0.004968
len_cd	len3u	-0.079376	2.29E-07	0.006301
len_cd	gc_c1	-0.163237	1.07E-26	0.026646
len_cd	gc_c3	-0.2974	2.71E-87	0.088447

Table S1-6. Hyper-parameters used with deep learning algorithms. CNN denotes convolutional neural networks, RNN recurrent neural networks and FC fully connected neural networks.

Type	Parameter name	Values	Value range
Global	num epochs	500	fixed
	early stopping min delta	0.01	fixed
	early stopping patience	50	fixed
	LRS* epoch drop	10	fixed
	learning rate	(0.00001,0.1)	log variable
	beta_1	(0.5,0.95)	uniform variable
	beta_2	(0.9,0.95)	uniform variable
	epsilon	1.00E-07	fixed
	mbatch	[64.128,256]	fixed
CNN	kernel size	[10, 20, 30, 40]	fixed
	filters	[32, 64, 128]	fixed
	dilation	[1, 2, 4]	fixed
	stride	1	fixed
	max-pool size	[1, 2, 4]	fixed
	max-pool stride	[1, 2]	fixed
	dropout	(0, 1)	uniform variable
RNN	kernel size	64	fixed
	dropout	(0, 1)	uniform variable
FC	dense size	[32, 64, 128]	fixed
	dropout	(0, 1)	uniform variable

* Learning rate scheduler

Table S2-1. Deep modeling results using different combinations of codon probabilities, mRNA stability variables and regulatory sequences.

Input variable combinations	**Target**	**Layer type**	**Input type**	**Train *R*²**	**Validation *R*²**	**Test *R*²**
Regulatory regions	TPM	CNN	Sequences	0.845	0.575	0.492
mRNA stability	TPM	Dense (FC)	8 variables	0.386	0.471	0.378
Coding regions	TPM	Dense (FC)	64 variables	0.715	0.742	0.69
Regulatory + stability	TPM	Dense (FC)	72 variables	0.597	0.603	0.558
Regulatory + coding	TPM	CNN + Dense	Seq. + 64 vars.	0.824	0.862	0.816
Codoning + stability	TPM	Dense (FC)	72 variables	0.721	0.751	0.755
All	TPM	CNN + Dense	Seq. + 72 vars.	0.841	0.87	0.822
Regulatory regions	Codon prob.	CNN + Dense	Sequences	0.538	0.543	0.582
Regulatory regions	Codon prob.	CNN + Dense	Sequences	0.969	0.776	0.779

Table S2-2. Shallow modeling results using linear regression with different combinations of codon probabilities, mRNA stability variables and kmers of size 4 to 6 as features.

Features	Kmer size	Train R^2	Test R^2	Train *MSE**	Test *MSE*	Fit time	Score time
codon_stability	4	0.699	0.685	0.039	0.040	0.030	0.002
codon	4	0.693	0.681	0.039	0.041	0.037	0.002
codon_stability_kmers	4	0.728	0.674	0.035	0.042	0.456	0.005
codon_kmers	4	0.720	0.667	0.036	0.043	0.470	0.007
stability_kmers	4	0.265	0.159	0.094	0.108	0.325	0.005
stability	4	0.147	0.142	0.109	0.110	0.002	0.001
kmers	4	0.153	0.031	0.109	0.124	0.409	0.005
codon_stability	5	0.699	0.685	0.039	0.040	0.077	0.002
codon	5	0.693	0.681	0.039	0.041	0.018	0.002
codon_stability_kmers	5	0.792	0.593	0.027	0.052	7.497	0.018
codon_kmers	5	0.788	0.585	0.027	0.053	6.992	0.016
stability	5	0.147	0.142	0.109	0.110	0.002	0.001
stability_kmers	5	0.423	-0.085	0.074	0.139	5.278	0.015
kmers	5	0.343	-0.234	0.084	0.158	6.558	0.018
codon_stability	6	0.699	0.685	0.039	0.040	0.057	0.002
codon	6	0.693	0.681	0.039	0.041	0.021	0.002
stability	6	0.147	0.142	0.109	0.110	0.002	0.001
codon_stability_kmers	6	1.000	-8.008	0.000	1.150	234.612	0.060
codon_kmers	6	1.000	-8.313	0.000	1.188	237.973	0.065
stability_kmers	6	1.000	-15.425	0.000	2.097	230.862	0.056
kmers	6	1.000	-17.296	0.000	2.333	235.376	0.068

* Mean squared error

Table S2-3. 14 yeast species used to analyse co-evolution of regulatory and coding regions.

Clade [29]	Species	Strain	Ensembl availability	Assembly
Saccharomyces	Saccharomyces cerevisiae	S288C	https://fungi.ensembl.org/Saccharomyces_cerevisiae/Info/Index	R64-1-1
Saccharomyces	Saccharomyces eubayanus	FM1318	http://fungi.ensembl.org/Saccharomyces_eubayanus_gca_001298625/Info/Index	SEUB3.0
	Candida glabrata	CSB 138	https://fungi.ensembl.org/_candida_glabrata_gca_000002545/Info/Index	ASM254v2
Kluyveromyces	Kluyveromyces lactis	NRRL Y-1140	http://fungi.ensembl.org/Kluyveromyces_lactis_gca_000002515/Info/Index	ASM251v1
Candida	Candida albicans	SC 5314	http://fungi.ensembl.org/Candida_albicans_sc5314_gca_000784635/Info/Index	Cand_albi_SC5314_V4
Candida	Debaryomyces hansenii	CBS767	http://fungi.ensembl.org/Debaryomyces_hansenii_cbs767_gca_000006445/Info/Index	ASM644v2
	Yarrowia lipolytica		http://fungi.ensembl.org/Yarrowia_lipolytica_gca_900087985/Info/Index	YALIA101
Schizosaccharomyces	Schizosaccharomyces pombe	972h-	http://fungi.ensembl.org/Schizosaccharomyces_pombe/Info/Index	ASM294v2
Schizosaccharomyces	Schizosaccharomyces japonicus	YFS 275	http://fungi.ensembl.org/Schizosaccharomyces_japonicus/Info/Index	GCA_000149845.2
	Saccharomyces kudriavzevii	IFO 1802	http://fungi.ensembl.org/Saccharomyces_kudriavzevii_ifo_1802_gca_000167075/Info/Index	Saccharomyces_kudriavzevii_strain_IFO1802_v1.0
	Saccharomyces arboricola	H-6	http://fungi.ensembl.org/Saccharomyces_arboricola_h_6_gca_000292725/Info/Index	SacArb1.0
	Saccharomyces sp boulardii	biocodex	http://fungi.ensembl.org/Saccharomyces_sp_boulardii__gca_001298375/Info/Index	ASM129837v2
	Kluyveromyces marxianus	DMKU3 1042	https://fungi.ensembl.org/Kluyveromyces_marxianus_dmku3_1042_gca_001417885/Info/Index	Kmar_1.0
	Kluyveromyces_dobzhanskii	CBS 2104	http://fungi.ensembl.org/Kluyveromyces_dobzhanskii_cbs_2104_gca_000820885/Info/Index	KLDO_01

Table S3-1. Construction of regulatory DNA motifs at different sequence identity cutoffs.

Seq. id.	Num. motifs	% Relevant sequences in motifs	% Jaspar targets	% Motif overlap between gene regions	Num. co-occuring motifs
0.8	2210	0.4401901474	0.318182	0.15268	116,734
0.85	2786	0.2716610804	0.284091	0.269168	12,809
0.9	1152	0.08214982063	0.210227	0.140091	408

Table S4-1. Groups of motif co-occurrence rules with a common Jaspar TFBS motif in promoter regions that define expression levels in an over 30 fold range of values.

Motif name	BH adj. *p*-value	Regions with differing motifs	Num. rules	Num. genes	Fold change
NHP6B	0.00448922	(3UTR, 5UTR, Promoter, Terminator)	144	144	648.016
ABF1	0.0499867	(3UTR, 5UTR, Promoter, Terminator)	32	42	298.673
STB3	0.000661653	(3UTR, 5UTR, Promoter, Terminator)	46	64	166.031
HAP3	0.0358934	(3UTR, 5UTR, Promoter, Terminator)	83	102	132.435
AZF1	0.0334191	(3UTR, 5UTR, Promoter, Terminator)	5	12	100.093
CBF1	0.0036968	(3UTR, 5UTR, Promoter, Terminator)	58	65	73.3709
CUP2	0.000975943	(3UTR, 5UTR, Promoter, Terminator)	3	21	55.2978
CUP9	0.022899	(3UTR, 5UTR, Promoter, Terminator)	54	77	53.2898
SFP1	0.00201301	(3UTR, 5UTR, Promoter, Terminator)	7	14	51.6828
RSC3	0.0423265	(3UTR, 5UTR, Promoter, Terminator)	10	17	42.2857
SUM1	0.0384774	(3UTR, 5UTR, Promoter, Terminator)	10	15	35.5945
NSI1	0.0178329	(3UTR, 5UTR, Promoter, Terminator)	18	29	34.9994

Supplementary References

1. Espinar, L., Schikora Tamarit, M. À., Domingo, J. & Carey, L. B. Promoter architecture determines cotranslational regulation of mRNA. *Genome Res.* **28**, 509–518 (2018).
2. Dvir, S., Velten, L., Sharon, E. & Zeevi, D. Deciphering the rules by which 5′-UTR sequences affect protein expression in yeast. *Proceedings of the* (2013).
3. Cuperus, J. T., Groves, B. & Kuchina, A. Deep learning of the regulatory grammar of yeast 5′ untranslated regions from 500,000 random sequences. *Genome* (2017).
4. Cheng, J., Maier, K. C., Avsec, Ž., Rus, P. & Gagneur, J. Cis-regulatory elements explain most of the mRNA stability variation across genes in yeast. *RNA* **23**, 1648–1659 (2017).
5. Shalem, O. *et al.* Systematic dissection of the sequence determinants of gene 3'end mediated expression control. *PLoS Genet.* **11**, e1005147 (2015).
6. Morse, N. J., Gopal, M. R., Wagner, J. M. & Alper, H. S. Yeast Terminator Function Can Be Modulated and Designed on the Basis of Predictions of Nucleosome Occupancy. *ACS Synth. Biol.* **6**, 2086–2095 (2017).
7. Lubliner, S. *et al.* Core promoter sequence in yeast is a major determinant of expression level. *Genome Res.* **25**, 1008–1017 (2015).
8. Sharon, E. *et al.* Inferring gene regulatory logic from high-throughput measurements of thousands of systematically designed promoters. *Nat. Biotechnol.* **30**, 521–530 (2012).
9. Redden, H. & Alper, H. S. The development and characterization of synthetic minimal yeast promoters. *Nat. Commun.* **6**, 7810 (2015).
10. Li, J., Liang, Q., Song, W. & Marchisio, M. A. Nucleotides upstream of the Kozak sequence strongly influence gene expression in the yeast S. cerevisiae. *J. Biol. Eng.* **11**, 25 (2017).
11. Zhou, Z., Dang, Y., Zhou, M., Yuan, H. & Liu, Y. Codon usage biases co-evolve with transcription termination machinery to suppress premature cleavage and polyadenylation. *Elife* **7**, (2018).
12. Watson, J. D. *et al. Molecular Biology of the Gene*. (Pearson/Benjamin Cummings, 2008).
13. Moqtaderi, Z., Geisberg, J. V., Jin, Y., Fan, X. & Struhl, K. Species-specific factors mediate extensive heterogeneity of mRNA 3′ ends in yeasts. *Proc. Natl. Acad. Sci. U. S. A.* **110**, 11073–11078 (2013).
14. Curran, K. A. *et al.* Short Synthetic Terminators for Improved Heterologous Gene Expression in Yeast. *ACS Synth. Biol.* **4**, 824–832 (2015).
15. Curran, K. A. *et al.* Design of synthetic yeast promoters via tuning of nucleosome architecture. *Nat. Commun.* **5**, 4002 (2014).
16. Neymotin, B., Ettorre, V. & Gresham, D. Multiple Transcript Properties Related to Translation Affect mRNA Degradation Rates in Saccharomyces cerevisiae. *G3* **6**, 3475–3483 (2016).
17. Ashburner, M. *et al.* Gene ontology: tool for the unification of biology. The Gene Ontology Consortium. *Nat. Genet.* **25**, 25–29 (2000).
18. The Gene Ontology Consortium & The Gene Ontology Consortium. The Gene Ontology Resource: 20 years and still GOing strong. *Nucleic Acids Research* **47**, D330–D338 (2019).
19. Keren, L. *et al.* Promoters maintain their relative activity levels under different growth conditions. *Mol. Syst. Biol.* **9**, 701 (2013).
20. Yamanishi, M. *et al.* A Genome-Wide Activity Assessment of Terminator Regions in Saccharomyces cerevisiae Provides a ″Terminatome″ Toolbox. *ACS Synth. Biol.* **2**, 337–347 (2013).

21. Jenjaroenpun, P. *et al.* Complete genomic and transcriptional landscape analysis using third-generation sequencing: a case study of Saccharomyces cerevisiae CEN. PK113-7D. *Nucleic Acids Res.* **46**, e38–e38 (2018).
22. Zeiler, M. D. & Fergus, R. Visualizing and Understanding Convolutional Networks. in *Computer Vision – ECCV 2014* 818–833 (Springer International Publishing, 2014).
23. Ancona, M., Ceolini, E., Öztireli, C. & Gross, M. Towards better understanding of gradient-based attribution methods for Deep Neural Networks. *arXiv [cs.LG]* (2017).
24. Salvador, S. & Chan, P. Toward accurate dynamic time warping in linear time and space. *Intelligent Data Analysis* **11**, 561–580 (2007).
25. Zhang, P. *et al.* Genome-wide mapping of nucleosome positions in Saccharomyces cerevisiae in response to different nitrogen conditions. *Sci. Rep.* **6**, 33970 (2016).
26. Huisinga, K. L. & Pugh, B. F. A genome-wide housekeeping role for TFIID and a highly regulated stress-related role for SAGA in Saccharomyces cerevisiae. *Mol. Cell* **13**, 573–585 (2004).
27. Khan, A. *et al.* JASPAR 2018: update of the open-access database of transcription factor binding profiles and its web framework. *Nucleic Acids Res.* **46**, D1284 (2018).
28. Teixeira, M. C. *et al.* YEASTRACT: an upgraded database for the analysis of transcription regulatory networks in Saccharomyces cerevisiae. *Nucleic Acids Res.* **46**, D348–D353 (2018).
29. Thompson, D. A. *et al.* Evolutionary principles of modular gene regulation in yeasts. *Elife* **2**, e01114 (2013).